LBL-31164
Preprint

# Lawrence Berkeley Laboratory
UNIVERSITY OF CALIFORNIA

## EARTH SCIENCES DIVISION

Submitted to Journal of Geophysical Research

# Effects of Periodic Atmospheric Pressure Variation on Radon Entry into Buildings

Y.W. Tsang and T.N. Narasimhan

October 1991

LOAN COPY
Circulates
for 4 weeks
Bldg. 50 Library.
LBL-31164
Copy 2

Prepared for the U.S. Department of Energy under Contract Number DE-AC03-76SF00098

## DISCLAIMER

This document was prepared as an account of work sponsored by the United States Government. While this document is believed to contain correct information, neither the United States Government nor any agency thereof, nor the Regents of the University of California, nor any of their employees, makes any warranty, express or implied, or assumes any legal responsibility for the accuracy, completeness, or usefulness of any information, apparatus, product, or process disclosed, or represents that its use would not infringe privately owned rights. Reference herein to any specific commercial product, process, or service by its trade name, trademark, manufacturer, or otherwise, does not necessarily constitute or imply its endorsement, recommendation, or favoring by the United States Government or any agency thereof, or the Regents of the University of California. The views and opinions of authors expressed herein do not necessarily state or reflect those of the United States Government or any agency thereof or the Regents of the University of California.

LBL-31164

# Effects of Periodic Atmospheric Pressure Variation on Radon Entry into Buildings

*Y. W. Tsang and T. N. Narasimhan*

Earth Sciences Division
Lawrence Berkeley Laboratory
University of California
Berkeley, California 94720

October 1991

This work was supported by the Director, Office of Energy Research, Office of Health and Environmental Research, Ecological Research Division, and by the Assistant Secretary for Conservation and Renewable Energy, Office of Building and Community Systems, Building Systems Division, of the U.S. Department of Energy under Contract No. DE-AC03-76SF00098.

# Effects of Periodic Atmospheric Pressure Variation on Radon Entry into Buildings

*Y. W. Tsang and T. N. Narasimhan*

Earth Sciences Division
Lawrence Berkeley Laboratory
University of California
Berkeley CA 94720

## ABSTRACT

We have investigated, using a mathematical model, the temporal variations of radon entry into a house basement in the presence of time dependent periodic variations of barometric pressure as well as a persistent small steady depressurization within the basement. The tool for our investigation is an integral finite difference numerical code which can solve for both diffusive and advective flux of radon in the soil gas which is treated as a slightly compressible fluid. Two different boundary conditions at the house basement are considered: (1) a dirt floor basement so that diffusion is equally or more important than advective transport and (2) an "impermeable" cement basement except for a 1 cm wide crack near the perimeter of the basement of the basement floor, in which case advective transport of radon flux dominates. Two frequencies of barometric pressure fluctuation with representative values of amplitudes, based on a Fourier decomposition of barometric pressure data, were chosen in this study: one with a short period of 0.5 hour with pressure amplitude of 50 Pa, the other a diurnal variation with a 24 hour period and the typical pressure amplitude of 250 Pa. For a homogeneous soil medium with soil permeability to air between $10^{-13}$ m$^2$ and $10^{-10}$ m$^2$, we predict that the barometric fluctuations increase the radon entry into the basement by up to 120% of the steady radon inflow into the basement due to a steady depressurization of 5 Pa. If soil permeability heterogeneity is present, such as the presence of a thin layer of higher permeability aggregate immediately below the basement floor, radon flux due to pumping is further increased. Effects of pressure pumping on radon entry is also compared to diffusion only transport when the steady depressurization is absent. It is found that contribution to radon entry is significant for the basement crack configuration. In particular, for pressure pumping at 0.5 hour period and for a homogeneous medium of permeability of $10^{-10}$ m$^2$, the radon entry is a factor of 10 larger than the diffusive transport. This may help to explain indoor radon concentrations during periods of low steady-state driving force.

## BACKGROUND

A necessary first step in seeking to manage radon levels in the indoor environment is to understand the phenomenon of radon entry into buildings. Studies so far [e.g. Sextro et al., 1987; Nazaroff and Nero, 1988] have shown that the soil adjacent to the house substructure is usually the dominant radon source in buildings with even moderately elevated radon concentrations. Radon is produced within the soil by the radioactive decay of radium, which is present in all earth-crustal materials, and is transported within the soil both by diffusion and advective flow of soil gas. At the soil-basement interface, radon enters the building through restricted openings (cracks, joints and holes). Existing data [Nazaroff et al., 1988; Nazaroff and Nero, 1988] indicate that high concentrations of indoor radon are usually associated with elevated rates of radon influx, advectively transported with the bulk soil gas inflow which is driven by small pressure differentials (of the order of a few pascals) between the basement and the land surface. The pressure differences are caused by indoor-outdoor temperature differences (stack effect), interaction of wind with the building envelope, and operation of exhaust fans.

It is noteworthy that though steady air inflow is dictated by pressure differences of but a few pascals, the transient barometric pressure fluctuations consist of periodic components with amplitudes ranging from a few Pa for periods of minutes, to a few hundred Pa in diurnal variations. Since these transient pressure variations have magnitudes equal or larger than the pressure difference which is responsible for steady airflow, the question arises as to the significance of the transient pressure variation to the radon entry rate into building. That decreasing atmospheric pressure causes an increase in exhalation of $^{222}Rn$ from soil surface, and an upward shift of its concentration profile in soil gas has been known for a long time (see review articles by Tanner, 1964; 1980). However, no general analytical treatment of the combined effects of diffusion and advection induced by atmospheric pressure changes appeared until that of Clements and Wilkening [1974]. They solved the advective diffusive differential equation involving radon production and decay by numerical methods to interpret their reported field data of radon fluxes across the earth-air interface in response to pressure changes of 1000-2000 Pa associated with the crossing of weather fronts. They observed that the instantaneous radon flux can vary from 20 to 60%. The magnitude of the radon flux in response to atmospheric pressure changes understandably will be a function of soil properties such as porosity, permeability and gas saturation. Indeed, Schery et al. [1982] reported that in a fractured rock

environment, the instantaneous radon flux can be increased by as much as an order of magnitude in response to similar decreases in atmospheric pressure as reported by Clements and Wilkening [1974]. However, since such atmospheric pressure variation is cyclical, oftentimes it is the time-averaged radon flux rather than the instantaneous radon flux that is of interest. Schery and Gaeddert [1982] reported the measurement of the time averaged radon flux as a result of natural pressure cycles such as due to the passage of cyclonic weather systems. Their measurements indicate a modest net enhancement of flux ($\approx$ 10%). Mathematical modeling of transient radon flux from soil and fractured rock surfaces in response to atmospheric pressure variations include those of Bates and Edwards [1980], Holford et al. [1989], and Owczarski et al. [1990]. Holford et al. use a two dimensional finite element code to simulate the radon fluxes from a dry, cracked soil. Owczarski et al. study the effect of varying the water content of five homogeneous soil types and atmospheric pressure on the transport of radon from soil surfaces. Thus, most of the work reported in the open literature concerns radon flux at the interface of atmospheric air with either soil or fractured rock column and involves fluid flow essentially in one-dimension. To our knowledge, little modeling work has appeared in the open literature regarding the effect of transient pressure variation to radon entry into buildings.

To date, modeling studies on radon entry into houses mostly focus on the steady state radon entry rate due to a slight under-pressure at the house basement. These studies include works of Scott [1983], Eaton and Scott [1984], DSMA [1985], Loureiro [1987], Mowris and Fisk [1988], Revzan and Fisk [1990], Revzan et al. [1991a, 1991b]. In order to investigate the potential importance of transient air flow to radon entry into buildings, we, in an earlier paper [Narasimhan et al, 1990] modeled the temporal variations of soil air flux into a basement caused by periodic variations in barometric pressure in the presence of a persistent under-pressure at the basement. Results of that study show that for a homogeneous soil medium, the effects of barometric fluctuation are most significant in the cases where soil permeability to air is low and the fluctuation frequency is high. In these cases, the barometric fluctuation can greatly enhance the magnitude of soil gas fluxes as well as introduce flow direction reversals from surrounding soil into the basement. Now, in this paper, we specifically investigate the radon entry into the basement in the presence of transient atmosphere pressure pumping.

## PROBLEM DEFINITION

To study the combined effects of time-dependent barometric fluctuations and time-independent under-pressure on soil gas inflow and radon entry at a basement, we define the problem as shown schematically in Figure 1. The water table lies 5 m below the land surface and 3 m below the 10-meter wide basement floor. In the absence of all driving forces except gravity, the soil air within the soil formation will be static if the gas pressure at each elevation, z, above the water table is $P_o(z) = \bar{P}_{wt} - \rho g z$ where $\bar{P}_{wt}$ is the mean air pressure at the water table, assumed throughout this work to be $10^5$ Pa, $\rho$ is the density of air and g is acceleration due to gravity. Pressure boundary conditions which would induce persistent air inflow into the basement were chosen as follows. The mean pressure $\bar{P}$ at the land surface is equal to $P_o$ (z = 5 m) and the mean pressure at the basement floor is assumed to be always 5 Pa below that at the land surface, $P_o$ (z = 3 m) − 5 Pa, thus insuring a continuous Darcy flow of soil gas into the basement. The fluctuations in the atmospheric pressure are assumed to be felt at both the land surface and at the basement floor with no damping or phase lag. For our initial studies, the atmospheric pressure fluctuations are assumed to consist of a single sinusoidal component with a given amplitude and frequency oscillating around the respective mean values of $\bar{P}$ at the outside land surface and the basement. Two different boundary conditions at the basement floor are implemented. One is an open boundary over the entire floor, this will be the case when the basement floor has no impermeable covering such as a concrete slab, referred hereafter to as the dirt floor basement. The other is a closed boundary except for a 1 cm opening centered at x=4.4 m (0.6m from the basement edge), which corresponds to a basement covered by an "impermeable" concrete slab except for a small penetration (cracks, joints, holes) that extend between the indoor and the soil.

## APPROACH

Because of the complex geometry of the soil-house interface, and the numerous processes that are involved (transient pressure driven gas flow, radon production and decay, diffusion and advection of radon), numerical models constitute a powerful tool for studying the proposed problem. For our calculations we use an isothermal fluid flow and chemical transport model CHAMP (Narasimhan et al., 1985). CHAMP solves mass balance equations that describe fluid and tracer mass flow in general multi-dimensional

system (1D, 2D or 3D). The numerical model can handle heterogeneous or anisotropic media; porous or fractured porous formations; time dependent boundary conditions and source terms. CHAMP is based on an "Integral Finite Difference Method" (Edwards, 1972; Narasimhan and Witherspoon, 1976) in which space discretization is made directly from the integral form of the basic conservation equations, without converting them into partial differential equations. This "Integral Finite Difference Method" avoids any reference to a global system of coordinates, and thus offers the advantage of being applicable to regular or irregular discretizations in one, two or three dimensions. It is particularly suited to arbitrary geometry and can handle mixed symmetry. For example, in the present problem of a small crack opening in the basement floor, the discretization is chosen to be radial in the immediate vicinity of the opening, but cartesian away from the crack opening (Figure 4). This kind of gridding which conform closely to the anticipated geometry of flow lines afford great improvement in the accuracy of numerical results [Narasimhan, 1985]. CHAMP has the option of either discretizing time explicitly as a forward first order difference, or fully implicitly as a first order backward finite difference. The implicit scheme is chosen for this study. The discretization of the mass conservation equations results in a set of algebraic equations, which are solved completely simultaneously with a sparse version of LU decomposition and backsubstitution (Duff, 1977). The code CHAMP was originally developed to solve problems of transient flow of water in isothermal, variably saturated, deformable media from one to three dimensions. Nevertheless, it can be readily applied to air flow in so far as air can be idealized as a slightly compressible fluid, where the ideal gas law is utilized to give the compressibility of air. This idealization is indeed appropriate in our case since we deal with pressure fluctuations of a fraction of a per cent of the mean pressure. In CHAMP, fluid flow is solved first, and then the transport at every time step. The assumption of one way coupling from flow to transport is based on the excellent approximation that transport of dilute species does not significantly affect the density of the fluid. This results in the solution of the problem in the form of two N×N matrices for N discretized nodes rather than in the form of a 2N×2N matrix. The flow portion of CHAMP is the numerical code TRUST, which has been extensively verified against analytical solutions and validated against numerous experimental results [e.g. Narasimhan and Witherspoon, 1978].

For verification of the accuracy of the numerical model CHAMP, the simulated results using CHAMP is compared to a 1D analytical solution of the advective-diffusive

equation with radioactive decay and a constant source term. The governing equation for the 1D problem is

$$\frac{\partial C}{\partial t} = D_d \frac{\partial^2 C}{\partial z^2} - \frac{v}{n}\frac{\partial C}{\partial z} - \lambda C + G, \tag{1}$$

with C = concentration of radon (Bq/m$^3$ of soil gas),

$D_d$ = bulk coefficient of diffusion of radon in soil, including soil porosity and tortuosity effects, (m$^2$/s),

v = Darcy velocity of soil gas (m/s),

n = porosity of the formation,

$\lambda$ = radioactive decay constant of radon ($2.1 \times 10^{-6}$ s$^{-1}$), and

G = rate of radon production in soil per unit volume of soil gas (Bq/m$^3$–s).

Boundary conditions are such that at the ground surface the concentration C(z=0) = 0 for all times, whereas deep into the formation $C_\infty$ ($z = -\infty$) is a constant, therefore,

$$\left.\frac{\partial C}{\partial z}\right|_{z=-\infty} = 0. \qquad \left.\frac{\partial^2 C}{\partial z^2}\right|_{z=-\infty} = 0. \tag{2}$$

We see that $C_\infty = G/\lambda$ by substituting (2) into (1) at steady state, $\frac{\partial C}{\partial t} = 0$. At steady state, the expression

$$C = C_\infty (1 - e^{mz}) \tag{3}$$

satisfies both boundary conditions at z = 0 and $z = -\infty$, and m is solved by substituting Eq (3) into Eq (1), then the steady state analytic solution for (1) is

$$C = \frac{G}{\lambda}\left[1 - \exp\left[\left[\frac{v}{2D_d n}\right] + \left\{\left[\frac{v}{2D_d n}\right]^2 + \frac{\lambda}{D_d}\right\}^{1/2}\right] z\right] \tag{4}$$

For the verification exercise, we model a 1D column of soil with uniform porosity and homogeneous permeability to air. A negative pressure is applied at the ground surface (z=10 m) with respect to the other end of the column (z=0 m) so that radon can move to the land surface by both advection and diffusion. Parameters values were chosen to resemble those which will be used in subsequent modeling of radon entry into houses, they are:

$D_d = 1.\times10^{-6} m^2/s$

v = $0.2778\times10^{-6}$ m/s, corresponding to the Darcy velocity of air with viscosity $1.8\times10^{-5}$ kg/m-s, through a 10 m soil column of permeability $10^{-11} m^2$, where an under-pressure of 5 Pa is applied at the ground surface.

n = 0.25

G = .1836 Bq/m$^3$-s, which derives from $G = f\rho_s(1-n)\lambda[Ra]/n$, with the typical values of soil grain density $\rho_s = 2650$ kg/m$^3$, emanation fraction f=.1, radon decay constant $\lambda = 2.1\times10^{-6} s^{-1}$, and the concentration of $Ra_{226}$ in soil grains [Ra] = 110 Bq/kg [Owczarski, 1990].

Figure 2 shows the verification of CHAMP simulation of radon concentration profile versus elevation with respect to the water table (elevation 10 m corresponds to the land surface). The solid line curve represents the analytical solution, Eq (4), while the dots correspond to the simulated radon concentration at discretized nodal points. The agreement is excellent. Note that rather coarse numerical grids ($\Delta z$=.2 m) near the land surface are adequate to reproduce the analytical results. On figure 2, we also show the verification of CHAMP for the case where the permeability of the soil column is increased 50-fold to $5\times10^{-10}$ m$^2$ to give the velocity v = $1.378\times10^{-5}$ m/s. In this case the dotted line is the analytical solution and the open circles are numerical predictions. Note that a much more refined discretization ($\Delta z$ = .02 m is needed to reproduce the very sharp profile of concentration near the soil surface. For both curves, we have used mid-stream weighting (0.5 for both the upstream and downstream node) for the numerical transport calculations.

We have also labeled the curves in Figure 2 by the numerical Peclet number $Pe = v\Delta z/nD$. It is well known that numerical dispersion becomes more problematic with "sharp fronts." In fact, when the numerical Peclet number Pe exceeds 2, oscillations behind the sharp front appear in the numerical simulation. The oscillations can be reduced to a smeared-out broadened front by increasing the weighting of the upstream node. In our modeling studies, the numerical Peclet number for each node is monitored to insure that our results are not adversely affected by numerical dispersion.

## MODELING STUDIES

We idealize the configuration shown in Figure 1 as a two-dimensional XZ planar region, with a unit thickness in the third dimension Y, and a YZ plane of symmetry bisecting the width of the basement at x=0. By symmetry, we need to model only the domain to the right of the plane of symmetry in Figure 1. The water table at z = 0 m is assumed to be a closed boundary impermeable to air while the land surface for (x > 5 m, z = 5 m) is an open boundary. The concrete-lined vertical wall of the basement at x = 5 m is assumed impermeable. Initially the system is assumed to be pneumostatic, with $P(z) = \bar{P}_{wt} - \rho g z$ for all z. Pressure boundary conditions are imposed on the land surface and on the basement floor (over the entire length of the basement for the case of dirt floor basement; and over only the 1 cm crack opening centered at x = 4.4 m) as already described earlier. The flow domain is discretized into 320 nodal volumes, in the case of the dirt floor basement (Figure 3), and 352 nodal volumes for the case of the impermeable basement with the 1 cm crack (Figure 4), around which fine grids with radial symmetry are employed. Figures 3 and 4 show nodes of discretization only up to x = 10 m, while the modeling in fact extends to x = 39 m, a closed boundary, with ever increasing $\Delta x$ as x increases. Soil porosity is assumed to be constant and air is prescribed a constant compressibility of $10^{-5}$ $Pa^{-1}$ from the ideal gas law at the reference pressure of $10^5$ Pa, a constant density of 1.21 $kg/m^3$ and a constant viscosity of $1.8 \times 10^{-5}$ kg/m-s. We are aware that in general air permeability will vary in space and in time due to soil heterogeneity as well as variations in water saturation. Yet, for these initial studies we consider a simplified system where the permeability is assumed not to vary with distance from the water table, and in most cases a homogeneous soil formation is assumed, where modeling studies are carried out with permeabilities ranging from $10^{-13}$ $m^2$ to $10^{-10}$ $m^2$ for both the dirt floor basement configuration as well as the impermeable basement floor with a 1 cm crack configuration. The only kind of permeability heterogeneity considered in this study is the special case where the permeability equivalent to a few orders of magnitude larger than the rest of formation characterize a thin layer of soil immediately below the basement floor. This corresponds to the physical situation where a porous sublayer of highly permeable aggregate is present below the basement floor. The permeability value chosen for this high permeability layer of thickness $\Delta z$=.4 m is $10^{-10}$ $m^2$. The layer's extent is represented by the shaded region in Figure 4.

Two frequencies with representative values of amplitudes (based on a Fourier decomposition of barometric pressure data) are chosen in this study of the dependence of air flow and radon entry on barometric pressure pumping. They are, (1) a short period of T=0.5 hour with pressure amplitude A=50 Pa, (2) a diurnal variation with a 24 hour period and the typical pressure amplitude of 250 Pa.

The calculations are carried out in two steps. First the steady state pressures, air fluxes, radon concentration and fluxes are obtained with only the constant under-pressure of 5 Pa imposed at the basement floor. Then the oscillating atmospheric pressure is incorporated and the response of the medium to the full set of pressure boundary conditions is calculated. The transport boundary conditions are such that radon concentration remains zero at the land surface and the basement opening (the entire basement floor for the dirt basement configuration and the 1 cm opening for the crack configuration). The simulations are run on a Cray X-MP computer, typically requiring the order of a few minutes of CPU time for a complete run with specified parameters. The results of calculations are summarized in Tables 1 and 2. The accuracy of the numerical code CHAMP is demonstrated in the fact that for the steady state calculations in the absence of pressure pumping, the mass of air entering the land surface boundary balances the mass of air entering the basement up to eight significant figures in all cases studied.

In order to get a handle on the relative importance of the diffusive, steady state advective, and pumping advective transport for the different basement configurations, calculations where no underpressure of 5Pa is imposed at the basement floor with respect to the outside land surface are also carried out. The results are summarized in Tables 3 and 4.

## RESULTS

Figure 5 shows the time varying oscillatory radon entry rate (the top four curves with reference to units on the left y axis) when the forcing function has a period of .5 hr; and the sinusoidal time variation of the pumping pressure (bottom curve with reference to units on the right y axis). Radon flow are shown for two cases: $k = 10^{-11}$ $m^2$ and $k = 10^{-12}$ $m^2$ for the dirt floor basement configuration. The steady radon entry rate into the basement in the absence of pressure pumping are represented by the two horizontal lines at -.29 Bq/s (for $k = 10^{-11}$ $m^2$) and -.178 Bq/s (for $k = 10^{-12}$ $m^2$). The – sign on the radon

fluxes simply indicates the direction of the radon flux is into the basement. Note that the pressure increases in the first half of the .5 hr period, causing the air to flow from the basement back into the soil formation. In the modeling, we impose at the basement the boundary condition that the radon concentration is zero, based on the implicit assumption that the air in the basement is quickly mixed to dilute the influx of radon. Hence the air that is flowing back from the basement into the soil formation effectively carries no radon, thus forcing the advective radon flux to go to zero for the first part of the pumping period in Figure 5. Since Figure 5 displays the total radon flow, which includes both the advective and diffusive contributions, hence for the first part of the pumping period, the radon flux into the basement is reduced as compared to the case where pressure pumping is absent. During the second part of the .5 hr pumping period, the pressure decreases below its mean value, hence the air flow from the soil column into the basement increases, carrying with it additional advective radon flux. If the radon flux is exactly in phase with the pumping pressure, then the radon entry will decrease for the first half and then increase for the second half of the pumping period. Note that this is not so, rather, there is a phase lag between the radon flow and the pressure variation. We can compare the total amount of radon entry into the basement for the cases with or without pressure pumping by estimating the area enclosed by the radon flux curve and the axis $x = 0$ in each period. Let the area enclosed by the horizontal line of the steady state radon flux and the axis $x = 0$ axis be $A_1$, the area enclosed by the oscillatory radon flux and the axis $x = 0$ be $A_2$. The percent increase in radon entry is defined as $(A_2 - A_1)/A_1 \times 100$ and will be provided in Tables 1 and 2 discussed subsequently.

Similar curves for radon entry into the basement with the 1 cm crack configuration is shown in Figure 6 for the formation permeabilities of $10^{-10}$ $m^2$ (solid curve) and $10^{-11}$ $m^2$ (dashed curve). Columns 5 and 6 in Table 2 show that in these cases, the steady state radon inflow is dominated by the advective flux, hence in the first part of pumping cycle where pressure is decreasing, the total inflow practically reduces to zero since there is negligible contribution from the diffusive radon inflow. Note again the radon flux lags in phase behind the pressure sinusoidal variation. Note also that the oscillatory radon flux reaches its equilibrium values only after several cycles of pumping, this is because the radon concentration around the crack opening becomes redistributed in response to the pressure pumping (greatly increase in the second part of the pumping cycle), thus giving rise to a large radon advective flux. On the other hand, diffusion is always operative, the

larger the concentration near the crack opening, the larger is the diffusive flux which tends to reduce the concentration near the crack. The coupling of the advective and diffusive processes causes the oscillatory flux to arrive at equilibrium values after several pumping cycles.

We add here that during different times in the pumping period for the larger permeability cases, the numerical Peclet number for the nodes near the basement opening sometimes exceed 2; however, simulation results of radon flow using mid-stream or totally up-stream weighting are indistinguishable, indicating that in spite of the numerical inaccuracy in the concentration profile behind the sharp front (oscillation for mid-stream weighting, broadened for up-stream weighting), the concentrations immediately adjacent to the basement opening seem accurate enough to give indistinguishable results in radon flow independent of the weighting scheme.

The simulation results for the dirt floor basement and the 1 cm crack configurations are summarized respectively in Tables 1 and 2. Tables 1 and 2 are organized as follows. The first column specifies the permeability to air, the second through fourth columns relate to soil gas flow, the fifth through eighth columns relate to radon entry. In particular, the second column gives the 'steady state' soil air flow into the basement, that is the air flux with only the -5 Pa of under-pressure present at the basement (in the absence of sinusoidal pressure pumping). With the sinusoidal pressure pumping, the air flux becomes oscillatory in time about the steady state value. Columns 3 and 4 list the ratio of the amplitude of the oscillatory soil air flow to the steady state value, for the pumping periods of .5 hr and 24 hr respectively. The fifth column lists the 'steady state' total radon flux into the basement, including both the advective and diffusive contributions. The sixth column gives contribution from only the diffusive radon flow into the basement, that is, the influx of radon in the absence of all pressure differences. The diffusive flux is of course independent of the permeability. The seventh and eighth columns list respectively the percentage increase in radon entry (with reference to column 5) into the basement from sinusoidal pressure pumping with oscillatory periods of .5 hr and 24 hr and amplitudes of 50 Pa and 250 Pa, respectively. Since the radon flux at the basement is oscillatory in time when pressure pumping is present, the percentage increase in radon entry over the constant steady state value are time averages as discussed earlier.

In studying Tables 1 and 2, we note that the magnitude of the oscillatory air flow from pressure pumping does not bear a direct relationship with its enhancement to radon inflow. This needs to be explained in terms of the physical processes involved in the air flow and radon transport. We begin with the air flow. In column 2 the steady state air flux is linearly dependent on the permeability of the soil gas, when the constant permeability of the formation increases by an order of magnitude the air flow into the basement also increase by one order of magnitude. The ratios in columns 3 and 4 for the increase of the amplitude of the oscillatory air flux at the basement opening are not easily interpreted because they result from the subtle interference of transient effects in response to the complex boundary conditions: oscillatory forcing pressure at both the land surface and basement opening. The oscillatory air flux in response to the oscillatory pressure forcing function bears a phase lag and an amplitude attenuation. The smaller the soil permeability, and the larger the distance from the pumping source, the greater the phase lag and amplitude attenuation. With the two dimensional geometry in our model, every point on the flow path will be at a different distance from the two pumping pressure sources (basement and the outdoor land surface), and thus have different interference of phases and amplitudes, giving rise to the net amplitude of air flux into the basement as recorded in columns 3 and 4. However, in the limit of very large permeability and long period in the forcing pressure, the effects of both phase lag and amplitude attenuation become negligible and the communication between the two boundaries approaches instantaneous. Then, for the set of boundary conditions chosen here, where pressure pumping is present at both boundaries, the oscillatory forcing functions play no net role in increasing the time average soil air flow, indeed, we see that in both Tables 1 and 2 the enhancement to air flow is minimal (less than 4%) for the following cases: $K=10^{-10}\ m^2$, T=.5 hr; and $K=10^{-10}\ m^2$ and $K=10^{-11}\ m^2$, T=24 hr. In the opposite limit, where the permeability is very low, and the forcing function has a short period, the effects of time lag and phase attenuation become very important so that the oscillatory air flux at the basement is essentially responding to the local boundary condition at the basement opening and not "seeing" the forcing function at the far boundary at the land surface. Then one would expect large enhancement of the amplitude of the oscillatory air flux. This is again borne out in Tables 1 and 2 by the trend of increasing ratios in columns 3 and 4 moving down the column as permeability decreases. Note also from column 2 of Table 1 and Table 2, that the steady state soil gas inflow into the much smaller 1 cm crack is 40-80% of the

soil gas inflow into the basement with a soil floor.

Columns 5 through 8 of Table 1 and 2 list the radon entry into the basement. In column 5, the steady state radon flow is dominated by the diffusion process in the lowest permeability case studied: ($10^{-13}$ $m^2$); for the other cases, the steady radon inflow increases as permeability increases because of the advective process. We note that the increase of radon entry into the basement due to atmospheric pumping is not directly proportional to the permeability. With high permeability soil there is large enhancement of radon inflow during that part of the cycle when the pumping pressure is decreasing, yet the radon inflow into the basement is forced to zero when the pressure is increasing. The steady state radon inflow from the basement depressurization alone in the absence of pumping also increases with permeability. Consequently the relationship between permeability and increase in radon entry is complex. It is in the intermediate permeability range when the steady state radon inflow is not too large, yet the enhancement in pumping advective radon inflow when the pressure is decreasing is appreciable that the largest percentage increase in radon entry over time is found. The largest predicted increases (for uniform soil permeability) are for the cases $k=10^{-11}$ $m^2$ and T=.5 hr in the dirt basement configuration, and $k = 10^{-12}$ $m^2$, T=24 hr in the crack configuration. Note that the increase in radon inflow is even more if a high permeability ($10^{-10}$ $m^2$) layer is present beneath the concrete slab. This kind of permeability heterogeneity maximizes the effect of the 'local' enhancement of the pumping advective radon transport at the basement opening, yet the effective permeability of the formation remains small since the high permeability layer constitute only a small fraction of the total volume, the small effective permeability ensures that steady state radon inflow due to basement depressurization remains small if the soil permeability is $\leq 10^{-12}$ $m^2$. Figure 7 shows the variation of radon flux with time at the basement crack opening for the case where the soil permeability is $10^{-13}$ $m^2$, the dotted curve is for a homogeneous medium while the solid curve is for the case where the permeability is $10^{-10}$ $m^2$ for a thin layer of thickness $\Delta z$=.4 m immediately below the basement slab. The horizontal lines again represent the respective steady state radon inflow. The increase of radon inflow when a large permeability exists in the immediate vicinity of the crack entry is very apparent.

That the largest increase (over steady state advective flow from a persistent 5 Pa under-pressure at the basement) in radon entry should occur for soil formation with overall low permeability except near the crack entry is of interest. Because the large

permeability near the crack opening constitutes only a very small fraction of the flow path from the outdoor land surface to the basement, the "effective" permeability remains very close to the low permeability of the formation, thus suppressing the steady Darcy flow from the persistent pressure difference between the basement and the outside land surface. This particular configuration of permeability variation corresponds to the real-life situation of a subslab aggregate layer. For the same reason, it is clear that a soil formation with overall high permeability except for a thin layer of low permeability beneath the outside land surface, due to decrease in soil gas saturation as a result of rainfall or irrigation, the "effective" permeability along the flow path from outdoor land surface to basement will remain high, giving rise to high steady state Darcy advected radon entry and thus minimizing the effects of enhancement to radon entry from pressure pumping. Indeed, our simulations of a case where the formation permeability is assigned the value $10^{-11}$ $m^2$ with a thin layer ($\Delta z$=.4m) of low permeability $10^{-14}$ $m^2$ below the land surface shows results indistinguishable from those when the low permeability layer is absent.

In Tables 1, 2 and Figures 5 through 7 the effects of pressure pumping on air flow and radon entry have been presented always with reference to the case where an under-pressure of 5 Pa is also present in the basement to drive a steady state Darcy gas flow. In fact, there are instances such as periods of low wind, or when the building is not heated in the summer that under-pressure may be absent and there is no steady state advective radon flow, yet the atmospheric pressure variation would still play a role to introduce transient advective radon inflow. Therefore we carry out calculations to study the radon entry into the basement from pressure pumping alone in the absence of a small persistent under-pressure at the basement. To give an idea of the relative magnitude of radon entry into the basement for the three processes: (1) radon entry by diffusion only, in the absence of persistent under-pressure and pressure pumping, (2) radon entry by diffusion and steady state advection from an under-pressure of 5 Pa, but in the absence of pressure pumping, and (3) radon entry by diffusion and advective transport as a result of the time varying pressure pumping, but in the absence of a persistent under-pressure at the basement. These are tabulated in Table 3 for the dirt floor basement configuration and Table 4 for the basement crack configuration. The entries for the last two columns in Tables 3 and 4 are the mean radon entry when averaged over a pumping time period. It is quite clear that in the dirt floor basement configuration the diffusive radon transport dominates in the absence of a persistent depressurization at the basement floor (note the small

difference between the entries in the fourth and fifth columns and the second column). The radon entry from pressure pumping is not appreciable for $k > 10^{-11}$ $m^2$ when compared with the other two entry processes (diffusion and steady state advection). On the other hand, for the basement crack configuration, the contribution to radon entry from pressure pumping is significant, particularly for the short pumping period of 0.5 hour, where the contribution from pressure pumping is respectively 4 and 10 times that from diffusion for $k = 10^{-11} m^2$ and $k = 10^{-10}$ $m^2$.

## SUMMARY AND CONCLUSION

We have investigated, using a mathematical model, the temporal variations of radon entry into a house basement in the presence of time dependent periodic variations of barometric pressure as well as a persistent small under-pressure at the basement. Cases studied include those with soil permeability to air ranging from $10^{-13}$ $m^2$ to $10^{-10}$ $m^2$. Study results show that for a homogeneous soil medium, the largest increase in radon entry (over steady state advective transport in the presence of a 5 Pa under-pressure at the basement) occurs for $k = 10^{-12}$ $m^2$ with the barometric variation of period T=24 hr and amplitude 250 Pa in the crack configuration. The increase is 120%. In the dirt floor configuration, the largest percentage increase is 68% over that of steady radon entry with 5 Pa under-pressure at the basement for $k=10^{-11}$ $m^2$ and pumping period of .5 hr. The increase in radon entry with pumping is further enhanced when there is a heterogeneity in permeability arising from the physical situation of a high permeability aggregate layer immediately below the basement floor.

In addition to comparing the effects of pressure pumping on radon entry to steady state radon transport from a persistent 5 Pa under-pressure in the basement, the effects of pressure pumping on radon entry is also compared to diffusion only transport, that is, when depressurization in the basement is absent. Here it was found that contribution to radon entry from transient pressure pumping can be significant for the basement crack configuration. In particular, for the pumping period of 0.5 hour and amplitude 50 Pa, and for a homogeneous medium of permeability $k=10^{-10} m^2$, the radon entry is a factor of 10 larger than the diffusive transport. These results indicate that barometric pumping may help to explain indoor radon concentration during periods of low steady-state driving force such as in the summer when the building is not heated. On the other hand, pressure

pumping contributes negligibly to the total radon entry in the dirt basement configuration where the diffusive transport dominates.

In this first attempt to investigate the effect of transient atmospheric pressure on the radon entry into a house basement, we have made some simplifying assumptions and idealizations, but we have chosen parameters and geometries that are likely to be encountered in actual conditions. The different configurations chosen (dirt floor basement and impermeable basement floor with crack) serve to demonstrate the relative importance of the difference transport processes: diffusive, steady state advective and pressure pumping advective. It is the subtle interplay of these processes that gives rise to the different magnitudes of radon entry as illustrated in Tables 1 through 4. The type of permeability heterogeneity chosen here: locally large permeability below the basement entry (which corresponds to the real-life situation of a subslab large permeability aggregate), give rise to the highest increase in radon entry (with respect to advective steady state transport alone from the 5 Pa under-pressure at the basement), by perhaps a factor of two, in response to barometric pressure pumping. However, since this occurs for cases with small overall permeabilities ($10^{-12}$ $m^2$ and $10^{-13}$ $m^2$), when the radon transport is dominated by the diffusive process, the effect is not large in magnitude. More significant is the result of advective radon transport from pressure pumping in the absence of a persistent underpressure at the basement, where the mean radon entry rate may be an order of magnitude larger than the diffusive transport for $k=10^{-10}$ $m^2$.

## ACKNOWLEDGMENT

We would like to thank Moshen Alavi of the Earth Sciences Division of LBL for help in modifying the computer code CHAMP. Discussions throughout the course of this work as well as careful review of the paper and helpful suggestions by W. Fisk and A. Gadgil of the Energy and Environment Division of LBL are gratefully acknowledged. This work was supported by the Director, Office of Energy Research, Office of Health and Environmental Research, Ecological Research Division, and by the Assistant Secretary for Conservation and Renewable Energy, Office of Building and Community Systems, Building Systems Division, of the U. S. Department of Energy, under contract DE-AC03-76SF00098.

## REFERENCES

Bates, R. C., and J. C. Edwards, Mathematical modeling of time dependent radon flux problems, *Second International Mine Ventilation Congress, pp. 412-419, Society of Mining Engineers of AIME, N. Y., 1980.*

Clements, W. E., and M. H. Wilkening, Atmospheric pressure effects on Rn-222 transport across the earth air interface, *J. Geophys. Res.*, 79(33), 5025-5029, 1974.

Duff, I. S., MA28 - A set of FORTRAN subroutines for sparse unsymmetric linear equations, AERE Harwell Report R8730, July 1977.

DSMA Atcon Ltd., A computer study of soil gas movement into basements, DSMA Atcon Ltd., Report 1389/1333. Dept. of Health and Welfare, Ottawa, Ontario, Canada, March 1985.

Eaton, R. S., and A. G. Scott, Understanding radon transport into houses, *Radiation Protection Dosimetry*, 7, 251-253, 1984.

Edwards, A. L., TRUMP: A computer program for transient and steady state temperature distributions in multidimensional systems, National Technical information Service, National Bureau of Standards, Springfield, VA, 1972.

Holford, D. J., S. D. schery, J. L. Wilson, and F. M. Phillips, Radon transport in dry cracked soil: Two-dimensional, finite element model, report PNL 7116, Pacific Northwest Laboratory, Richland, WA., 1989.

Loureiro, C. O., Simulation of the steady state transport of radon from soil into houses with basements under constant negative pressure, Lawrence Berkeley Laboratory Report, LBL-24378, Berkeley, CA., 1987.

Mowris, R. J., and W. J. Fisk, Modeling the effects of exhaust ventilation on $^{222}$Rn entry rates and indoor $^{222}$Rn concentrations, *Health Physics*, 54, 491-501, 1988.

Narasimhan, T. N., Geometry - imbedded Darcy's law and transient subsurface flow, *Water. Resour. Res.*, 21(8), 1285-1292, 1985.

Narasimhan, T. N., and P. A. Witherspoon, An integrated finite difference method for analyzing fluid flow in porous media, *Water Resour. Res.*, 12(1), 57-64, 1976.

Narasimhan, T. N., and A. L. Edwards, and P. A. Witherspoon, Numerical model for saturated-unsaturated flow in deformable porous media: 2. The Algorithm, *Water Resour. Res.*, 14(2), 255-261, 1978.

Narasimhan, T. N., and P. A. Witherspoon, Numerical model for saturated-unsaturated flow in deformable porous media: 3. Applications, *Water Resour. Res.*, 14(6), 1017-1034, 1978.

Narasimhan, T. N., M. Alavi, and C. W. Liu, CHAMP - A computer code for modeling transient fluid flow and chemical transport with hydrodynamic dispersion in variably saturated systems, in Proceedings of the symposium on groundwater flow and transport modeling for performance assessment of deep geologic disposal of radioactive waste: A critical evaluation of the state of the art, Albuquerque, NM, May 20-21, 1985.

Nazaroff, W. W., H. Feustel, A. L. Nero, K. L. Revzan, and D. T. Grimsrud, Radon transport into a detached one-story house with a basement, *Atmospheric Environment,* 19(1), 31-46, 1985.

Nazaroff, W. W., S. R. Lewis, S. M. Doyle, B. A. Moed, and A. V. Nero, Experiments on pollutant transport from soil into residential basements by pressure-driven airflow, *Environmental Science & Technology,* 21, 459-466, 1987.

Nazaroff, W. W., and A. V. Nero, Jr., Editors, *Radon and Its Decay Products in Indoor Air,* J. Wiley & Sons, Inc., New York, 57-111, 1988.

Nazaroff, W. W., B. A. Moed, and R. G. Sextro, Soil as a source of indoor radon: generation, migration, and entry, in Radon and its decay products in indoor air, Ed. by W. W. Nazaroff and A. V. Nero, Jr., J. Wiley & Sons, Inc., New York, 57-111, 1988.

Owczarski, P. C. , D. J. Holford, H. D. Freeman, and G. W. Gee, Effects of changing water content and atmospheric pressure on radon flux from surfaces of five soil types, *Geophys. Res. Lett.,* 17(6), 817-820, 1990.

Revzan, K. L., and W. J. Fisk, Modeling radon entry into houses with basements: the influence of structural factors, Lawrence Berkeley Report, LBL-28109, Berkeley, CA., Submitted to *Indoor Air.*

Revzan, K. L., W. J. Fisk, and A. J. Gadgil, Modeling radon entry into houses with basements: model description and verification, *Indoor Air* 1(2), 173-189, 1991a.

Revzan, K. L., W. J. Fisk, and R. G. Sextro, Modeling radon entry into houses with concrete block stemwalls, Lawrence Berkeley Laboratory Report, LBL-30005, Berkeley, CA., 1991b. 1(2), 173-189, 1991a.

Scott, A. G., Computer modeling of radon movement, in EML indoor radon Workshop, Edited by A. C. George, W. Lowder, I. Fisenne, E. O. Knutson, and L. Hinchcliff, Report EML-416, Environmental Measurements Laboratory, New York, 1982.

Sextro, R. G., B. A. Moed, W. W. Nazaroff, K. L. Revzan, and A. V. Nero, Investigations of soil as a source of indoor radon, American Chemical Society Symposium Series No. 331, "Radon and its decay products" Ed. by P. L. Hopke, published by American Chemical Society, Washington D.C., 1987.

Schery, S.D., and D. H. Gaeddert, Measurement of the effect of cyclic atmospheric pressure variation on the flux of $^{222}$Rn from the soil, *Geophys. Res. Let.,* 9(8), 835-838, 1982.

Schery, S. D., D. H. Gaeddert, and M. H. Wilkening, Transport of radon from fractured rock, *J. Geophys. Res.,* 87(B4), 2969-2976, 1982.

Tanner, A. B., Radon migration in the ground: A review, in *The Natural Radiation Environment,* 161-190, University of Chicago Press, Chicago, Ill., 1964.

Tanner, A. B., Radon migration in the ground: A supplementary review, in *The Natural Radiation Environment III,* 5-56, Technical Information Center, U. S. Department of Energy, Springfield, VA., 1980.

Weeks, E. P., Field determination of vertical permeability to air in the unsaturated zone, U. S. Geological Survey Professional Paper 1051, U. S. Government Printing Office, Washington, 1978.

## Table 1.
## Air flow and radon entry at dirt floor basement with constant under-pressure of 5 Pa in the absence or presence of barometric pumping

| soil k ($m^2$) | Air flux (Kg/s) | | | Radon Entry (Bq/s) | | | |
|---|---|---|---|---|---|---|---|
| | Steady state | Ratio of Oscillatory amplitude to steady state | | Steady state | | % increase of radon entry with pressure pumping | |
| | | T=.5 hr A=50 Pa | T=24 hr A=250 Pa | Diffusive + advective | Diffusive alone | T=.5 hr A=50 Pa | T=24 hr A=250 Pa |
| $10^{-10}$ | $.269\times10^{-4}$ | 3.1 | .32 | .985 | .167 | 17. | ≤0. |
| $10^{-11}$ | $.269\times10^{-5}$ | 25. | 3.2 | .290 | .167 | 68. | 1. |
| $10^{-12}$ | $.269\times10^{-6}$ | 73. | 32. | .178 | .167 | 27. | 6. |
| $10^{-13}$ | $.269\times10^{-7}$ | 208. | 197. | .168 | .167 | 6. | 2. |

## Table 2.
## Air flow and radon entry at basement crack with constant under-pressure of 5 Pa in the absence or presence of barometric pumping

| soil k ($m^2$) | Air flux (Kg/s) | | | Radon Entry (Bq/s) | | | |
|---|---|---|---|---|---|---|---|
| | Steady state | Ratio of Oscillatory amplitude to steady state | | Steady state | | % increase of radon entry with pressure pumping | |
| | | T=.5 hr A=50 Pa | T=24 hr A=250 Pa | Diffusive + advective | Diffusive alone | T=.5 hr A=50 Pa | T=24 hr A=250 Pa |
| $10^{-10}$ | $.107\times10^{-4}$ | 2.9 | 0.3 | .520 | .011 | 10. | .5 |
| $10^{-11}$ | $.107\times10^{-5}$ | 12. | 3.1 | .075 | .011 | 38. | 6. |
| $10^{-12}$ | $.107\times10^{-6}$ | 15. | 28. | .015 | .011 | 31. | 120. |
| $10^{-12}$ + | $.259\times10^{-6}$ | 29. | 28. | .022 | .011 | 78. | 190. |
| $10^{-13}$ | $.107\times10^{-7}$ | 17. | 64. | .011 | .011 | 1. | 32. |
| $10^{-13}$ + | $.263\times10^{-7}$ | 41. | 131. | .012 | .011 | 31. | 198. |

+ With a 0.4 m thick layer of aggregate ($k=10^{-10}$ $m^2$) beneath the basement slab.

## Table 3.
## Radon entry at dirt floor basement for (1) diffusion (2) diffusion plus steady state advection (3) diffusion plus transient pressure pumping

| k ($m^2$) | Radon Entry (Bq/s) | | | |
|---|---|---|---|---|
| | Diffusion only | Diffusion + Advection with 5 Pa under pressure | Diffusion + Pressure pumping with no 5 Pa under pressure | |
| | | | T=.5 hr | T=24 hr |
| $10^{-10}$ | .167 | .985 | .182 | .177 |
| $10^{-11}$ | .167 | .290 | .169 | .177 |
| $10^{-12}$ | .167 | .178 | .172 | .177 |
| $10^{-13}$ | .167 | .168 | | |

## Table 4.
## Radon entry at basement crack for (1) diffusion (2) diffusion plus steady state advective (3) diffusion plus transient pressure pumping

| soil k ($m^2$) | Radon Entry (Bq/s) | | | |
|---|---|---|---|---|
| | Diffusion only | Diffusion + Advection with 5 Pa under pressure | Diffusion + Pressure pumping with no 5 Pa under pressure | |
| | | | T=.5 hr | T=24 hr |
| $10^{-10}$ | .0105 | .52 | .105 | .03 |
| $10^{-11}$ | .0105 | .075 | .045 | .03 |
| $10^{-12}$ | .0105 | .015 | .0125 | .025 |
| $10^{-13}$ | .0105 | .011 | | .0176 |

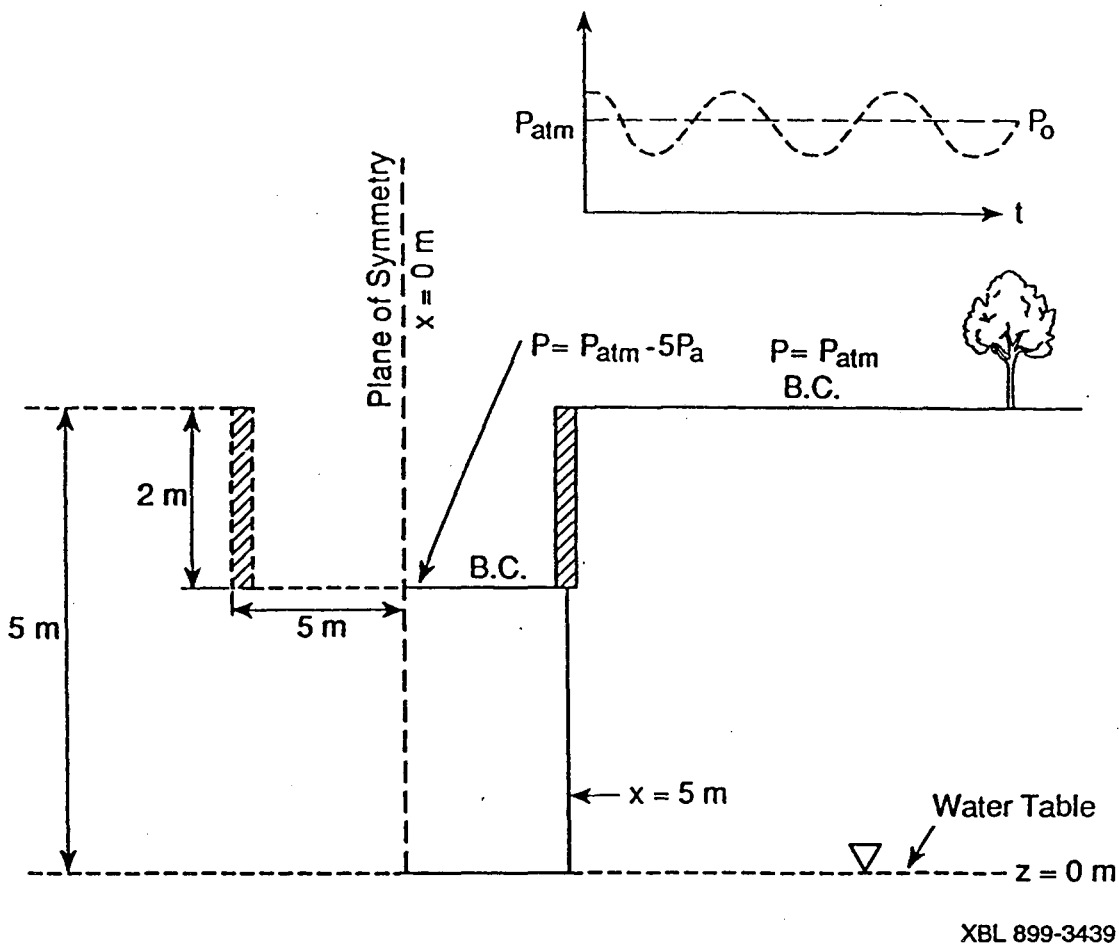


Figure 1 Schematic diagram for the basement configuration and pressure boundary conditions for modeling radon entry.

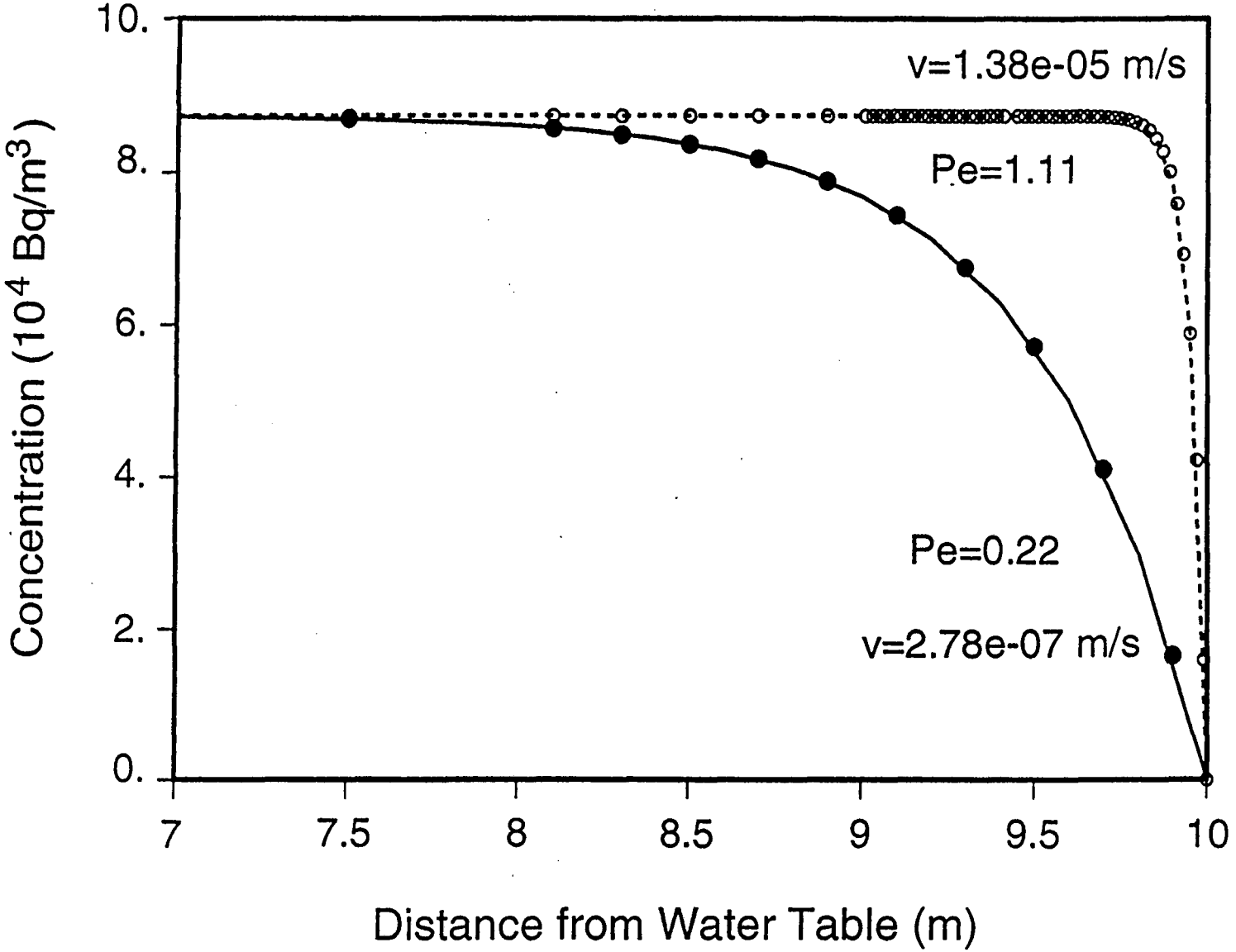


XBL 9110-6105

Figure 2 Verification of Simulated result from intergral finite difference code CHAMP for a 1D problem involving advection, diffusion, radon source and decay for (a) v = 2.78e-07 m/s, (b) v = 1.38e-05 m/s.

XBL 9110-6106

Figure 3 Integral Finite difference nodal points for the dirt floor basement configuration.

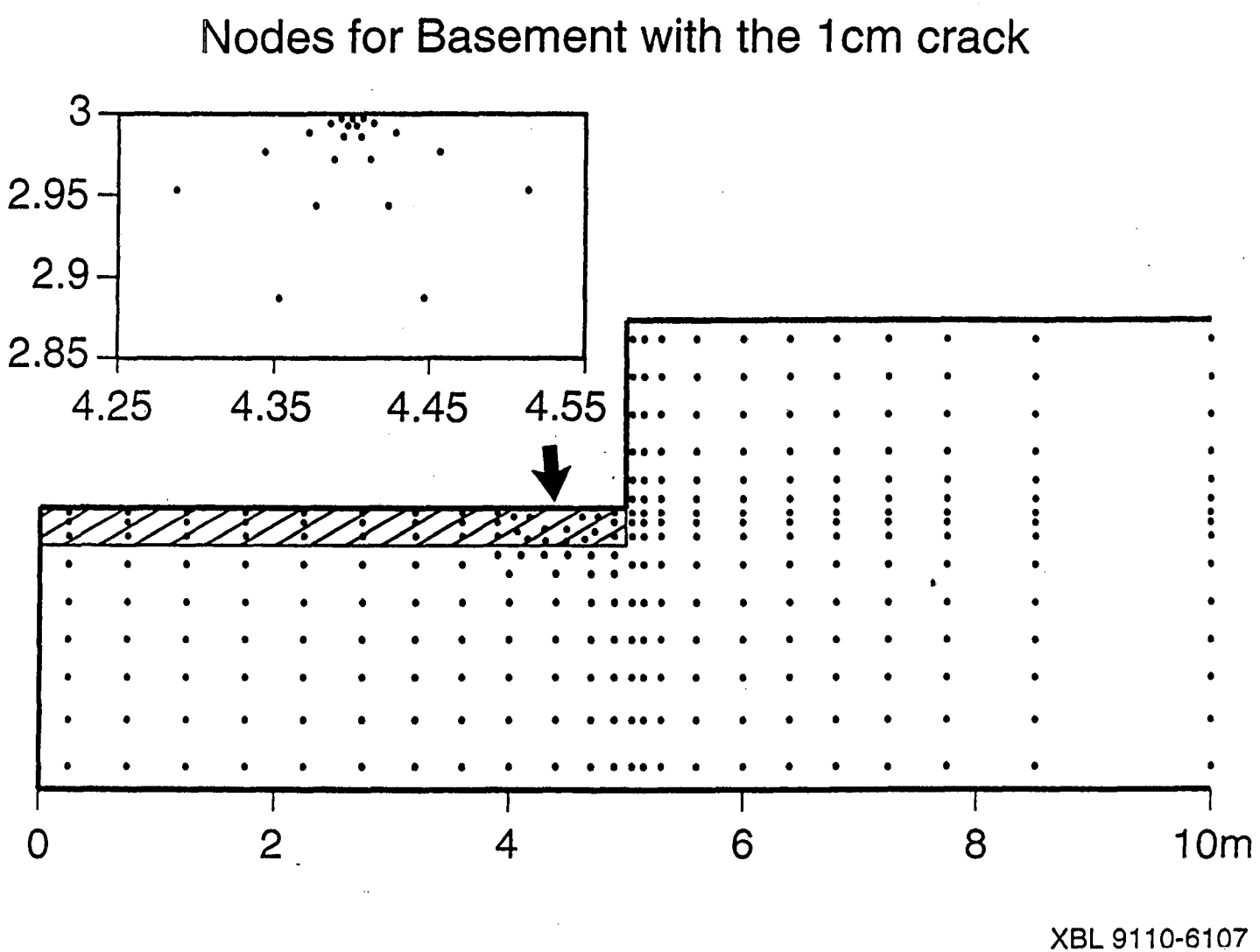


Figure 4 Integral Finite difference nodal points for the basement with 1 cm crack configuration. The shaded area corresponds to the subslab layer of high permeability aggregate.

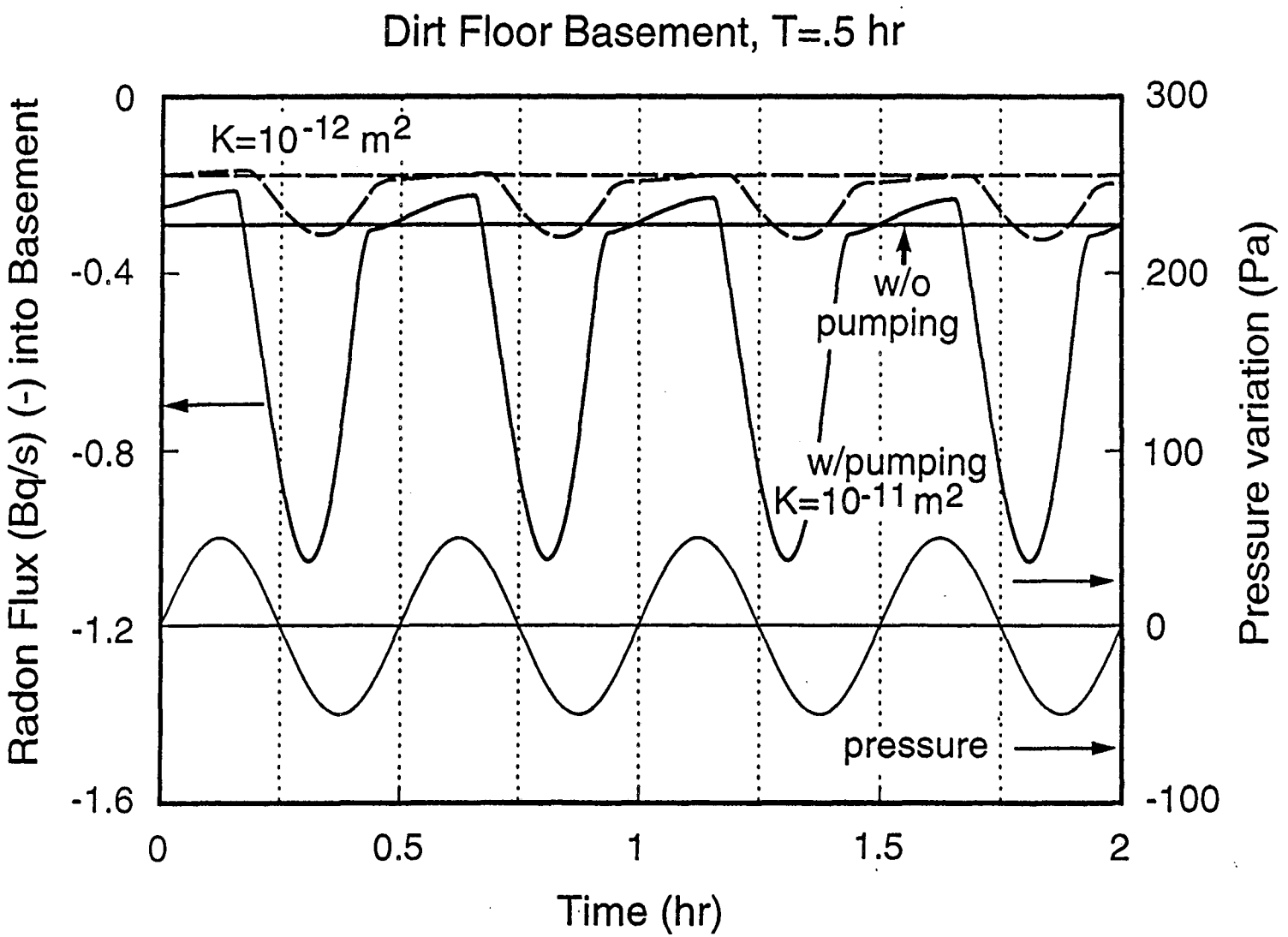


Figure 5 Radon inflow into the dirt floor basement with and without pressure pumping of T=.5 hr, for permeabilities $10^{-11}$ m$^2$ and $10^{-12}$ m$^2$; and pressure variation with time.

XBL 9110-6108

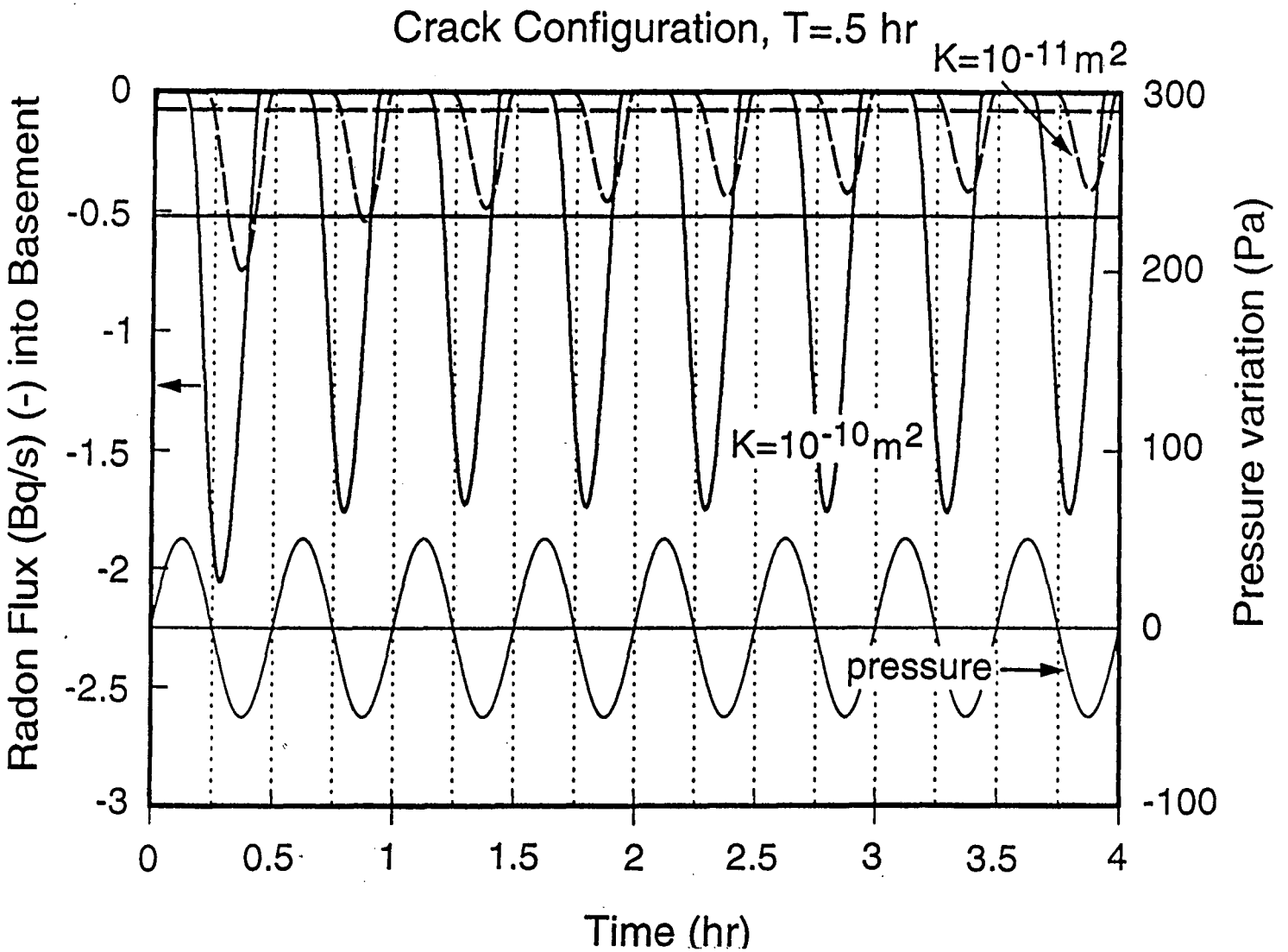


Figure 6 Radon inflow into basement crack with and without pressure pumping of T=.5 hr, for permeabilities $10^{-10}$ $m^2$ and $10^{-11}$ $m^2$; and pressure variation with time.

XBL 9110-6109

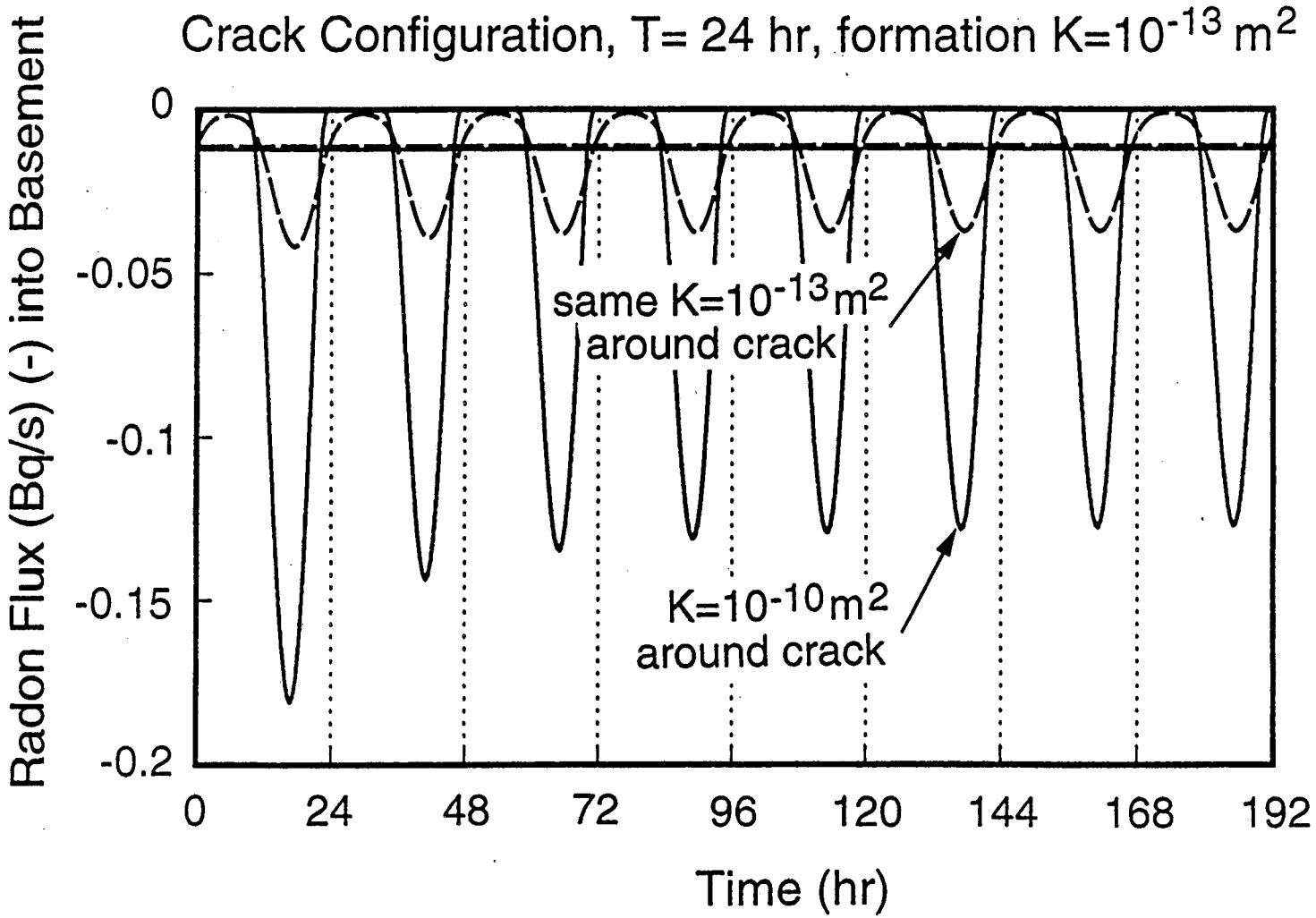


FIgure 7 Radon inflow into basement crack with and without pressure pumping of T=24 hr, the formation permeability is $10^{-13}$ $m^2$, the solid curves denotes the case where a subslab layer of aggregate with permeability $10^{-10}$ $m^2$ is present.

XBL 9110-6110

LAWRENCE BERKELEY LABORATORY
UNIVERSITY OF CALIFORNIA
INFORMATION RESOURCES DEPARTMENT
BERKELEY, CALIFORNIA 94720